EXPERIMENTAL AND NUMERICAL INVESTIGATION OF THE EFFECT OF VARIABLE OPERATING CONDITIONS ON PEMFC PERFORMANCE

by

Huseyin KAHRAMAN*

Department of Mechanical Engineering, Sakarya University of Applied Sciences, Sakarya, Turkey

Original scientific paper
https://doi.org/10.2298/TSCI2304089K

The operating parameters have an important impact on the performance of a proton exchange membrane fuel cell (PEMFC). This paper investigates experimentally and numerically the cell temperature and relative humidity which have a significant influence on the PEMFC current density. These parameters are adjusted simultaneously and dynamically during operation. A 50 cm^2 active area single-cell PEMFC with serpentine flow channel was studied. In order to confirm the experimental measurements, a mathematical model was established using the MATLAB package program and the results were compared. According to both experimental and mathematical model results, adjusting the operation parameters instantly according to the current value produced by the cell had a positive effect on the cell durability and performance.

Key words: *fuel cells, PEMFC, dynamic operating conditions, mathematical modeling*

Introduction

Industrialization, population growth and development in technology increase the energy demand of humanity day by day. Fossil fuel reserves, which have been used to meet the energy needs of humanity for many years, are gradually decreasing [1, 2]. On the other hand, the damage to the environment caused by the harmful gases released into the atmosphere as a result of the use of fossil fuels shows itself mostly as global warming [3, 4]. For this reason, worldwide research has focused on using RES and increasing energy efficiency [5]. Among alternative energy sources, fuel cells, especially polymer electrolyte membrane or PEM fuel cells, have been shown as an alternative to internal combustion engines in recent years due to their advantages such as high efficiency, zero emissions, fuel flexibility and modularity [6]. Fuel cells convert chemical energy into electrical energy using oxidizing agents such as hydrogen, methanol or natural gas [7]. There are many parameters that affect the PEMFC efficiency. Many design parameters such as flow channel designs [8-10], cell design [11-13], and stack configuration [14-16] affect the cell output performance, as well as the operational parameters that directly affect the chemical reaction mechanisms of the cell. Inside of a PEMFC stack, operating conditions are closely related with physical and chemical reactions such as gas diffusion, dissolution, absorption, departure, and precipitation. [17]. Adjusting the operating conditions at optimum values according to the current drawn from the fuel cell is a very

* Author's, e-mail: huseyink@subu.edu.tr

important issue for increasing efficiency. The first parameters that come to mind when operating conditions in fuel cells are mentioned: temperature (cell and reactant temperatures), operating pressure, stoichiometry, and relative humidity (RH) of the reactants [18]. Many operational parameters in fuel cells involve complex behaviors. When the behavior of the fuel cell is examined in the face of changing operating conditions, it is known that mathematical models are sometimes insufficient. It would be beneficial to use an ANN approach in addition to the mathematical model, especially when the changes in operating conditions are analyzed simultaneously.

Many studies have showed that, the effect of various factors on the output voltage of the stack discovering current density can influence the stability of the output voltage. The electrochemical reaction that takes place in PEMFC is an exothermic reaction that produces heat. Operating temperature is an important factor affecting the life of membranes and catalysts from PEMFC components. The optimum temperature increases the reaction rate, reduces the polarization voltage, which means the reduction of activation losses, improves the conversion efficiency. On the other hand, high temperature increases the water vapor pressure of the membrane, which will cause water loss and damage to the PEMFC [19]. In order to experimentally validate the polarization curve and temperature distribution in a PEMFC stack, Salva *et al.* [20] used a 1-D simulation. Kim *et al.* [21] measured the effects of cathode channel size and stack temperature on the oxygen and water concentrations and polarization resistance. The result reveals that current density and activation losses are significantly influenced by the cell temperature. Performance of the PEMFC fuel cell depends on water management. A fuel cell's performance and efficiency can be enhanced by maintaining an ideal humidity ratio, which can possibly prevent the degradation of internal components like catalysts and membrane [22]. Finding the best method to regulate water distribution and improve water management in PEMFC, many researchers have studied on CFD method. Santarelli and Torchio [23] examined how operation factors affected a single cell performance under various loads. They claimed that raising the operating temperature and RH improved the performance of the cell. Hu *et al.* [24] analyzed a CFD model to examine the effects of various parameters of catalyst layer and RH on PEMFC performance. They observed that increasing both anode and cathode reactants RH enhanced cell performance. Another study conducted by Wang *et al.* [25], to study the membrane and liquid water transport properties as well as cell performance with the co-flow and counter-flow configurations under various reactant RH values, they used a three-dimensional multiphase model. According to their findings, a lower anode RH with a cathode RH of 100% or a lower cathode RH with an anode RH of 100% results in a decrease in cell performance at high operational voltages and an increase in cell performance at low operational voltages. These results show that the same operating conditions cause different results at different values of the cell voltage. Therefore, it is of great importance to adjust the operating conditions instantly according to the current density/cell voltage.

Compared with the previous work, the effect of the mentioned conditions on PMFC performance is investigated both experimentally and mathematically in this article. Instead of testing the fuel cell with constant operating conditions, the conditions were changed dynamically during operation according to the current drawn from the fuel cell.

Experimental

All experiments in this work used a single PEM fuel cell with an active surface area of 50 cm^2. The Nafion® HP membrane and 45 wt.% Pt/C catalyst layers used in the MEA had loadings of 0.2 and 0.4 mg Pt/cm^2 on the anode side and cathode side, respectively. The MEA

were made using Pt/C catalyst particles that were made using a modified sodium borohydride reduction technique. Using the screen-printing technique, a homogenous coating of a semiliquid catalyst combination consisting nafion, Pt/C catalyst, water, isopropanol, and propanediol was applied to teflon sheets. During the screen-printing process, a silk screen with a mesh size of 100 was masked to a 50 cm^2 active region. Under around 20 Bar pressure and 130 °C temperature, coatings were applied on nafion HP using the decal transfer method to manufacture the MEA. All experiments made use of AvCarb EP40 GDL that were 200 microns thick.

As shown in fig. 1 electronic load bank, a multiple temperature controller, two mass flow controllers, two humidifier bottles, two heated gas lines, two pressure regulators, two ball valves serving as humidifier bypass valves, H_2 and O_2 bottles, and two backpressure regulators are all part of the experiment set-up. Table 1 shows the varying operating parameters.

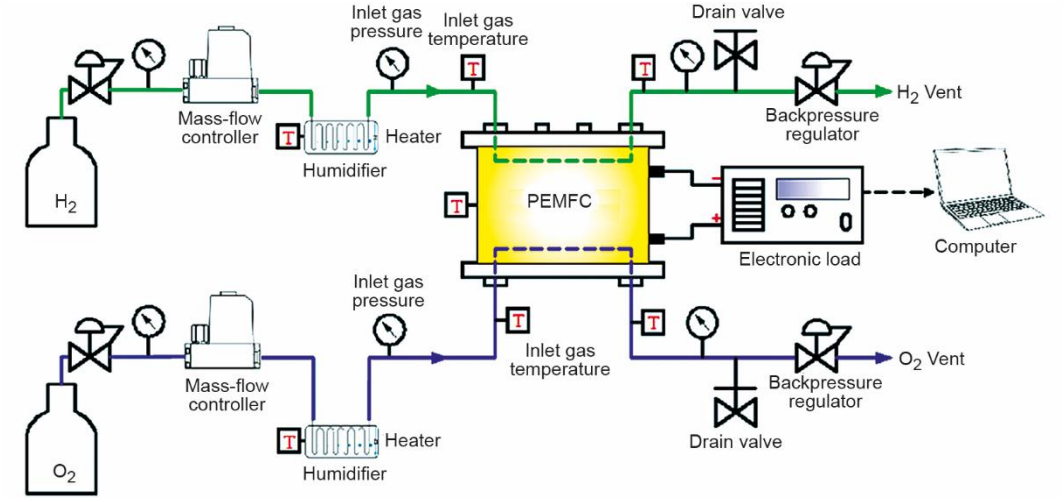

Figure 1. Experimental set-up

The 1 mm diameter carbide end mills were used to machine the 3 mm thick bipolar plates. Both surfaces of the graphite plates were thoroughly cleaned with a big tool before the channels were machined to enable homogenous compression across the MEA/GDL and prevent gas leakage. Compression was conducted using aluminum-manufacturing end plates, while current collectors were made of copper plates that were 300 microns thick and gold-plated. Serpentine flow design was preferred for all experiments.

Table 1. Dynamically changed operation parameters values

Operating parameter	Unit	Range of change
Cell temperature	[°C]	40-80
*Anode humidity bottle temperature	[°C]	40-80
*Cathode humidity bottle temperature	[°C]	40-80
Anode RH	[%]	0-100
Cathode RH	[%]	0-00

* While adjusting the RH of the reactant gases sent to the fuel cell, the heater of the humidity bottle and the related line was kept at the same temperature

While obtaining polarization curves, SINGLE CELL TEST PROTOCOL of US Fuel Cell Council was used as a reference test protocol. Before all measurements;

– For 20 minutes, the stack was maintained at open-circuit voltage.
– For the fuel cell to reach a steady state, 20 A was applied for 30 minutes.

Model governing equations

The mathematical model of the laminar, unsteady, two-phase flow is modelled by using MATLAB R2013a. In fuel cell modeling, the following assumptions are made:

– ideal gas characteristics,
– the fluid is incompressible,
– laminar flow,
– electrolyte, electrode, and bipolar material architectures that are homogeneous and isotropic,
– the ohmic potential drop of components are negligible, and
– using volume-averaged conservation equations, the macro perspective of mass and energy flow is modeled.

The conservation of mass [26] and momentum equations have been applied to the model. The continuity equation for the flow of a fluid with density ρ [kgm^{-3}], velocity v [ms^{-1}], ∇ – the operator, d/dx + d/dy + d/dz, and S_m – the additional mass sources and no source or sink terms may be written:

$$\frac{\partial \rho}{\partial t} + \nabla(\rho v) = S_\mathrm{m} \tag{1}$$

The conservation of momentum [27] equation is:

$$\frac{\mathrm{d}(\rho v)}{\mathrm{d}t} + \nabla(\rho v) = -\nabla p + \nabla(\mu_\mathrm{mix} \nabla v) + S_\mathrm{m} \tag{2}$$

where p [Pa] is the fluid pressure, μ [kgm^{-1}s^{-1}] – the viscosity, and S_m – the momentum source. This momentum source term varies in different parts of the fuel cell. Temperature has a significant impact on reaction rate. By resolving the energy conservation equation, it is crucial to consider temperature fluctuations within the cell. Equation (3) for any domain in a fuel cell describes the energy conversation [28]:

$$(\rho c_p)\frac{\mathrm{d}T}{\mathrm{d}t} + (\rho c_p)(v \nabla T) = \nabla(k_\mathrm{eff} \nabla T) + S_\mathrm{e} \tag{3}$$

where c_p [Jkg^{-1}K^{-1}] is the average specific heat capacity of mixture, T [K] – the temperature, thermal conductivity is denoted by k [Wm^{-1}K^{-1}], and S_e – the energy source term. The term for an energy source is S_e. The S_e considers reactional heat, ohmic heat, and phase change heat. For each reactant, the species balance equation indicates mass conservation. The gas phase's species conservation is [29]:

$$\frac{\partial(\varepsilon \rho x_i)}{\partial t} + \nabla(\varepsilon \rho x_i) = (\nabla \rho D_i^\mathrm{eff} \nabla x_i) + S_{\mathrm{s},i} \tag{4}$$

where D^eff is a function of porosity, $S_{\mathrm{S},i}$ – the additional species sources, and x_i – the mass fraction of the gas species. Back diffusion and electro osmotic drag are the two types of water

flux that exist in the Nafion membrane. The following equation can be used to account for both fluxes [30]:

$$J_{\mathrm{H_2O}}^{\mathrm{M}} = 2n_{\mathrm{drag}} \frac{i}{2F} \frac{\lambda}{22} - \frac{\rho_{\mathrm{dry}}}{M_m} D_\lambda \frac{\mathrm{d}\lambda}{\mathrm{d}z} \tag{5}$$

In the equation, the water content is not constant (5). The water content can be used to assess the electrolyte resistance.

In fuel cells, temperature is also a factor that changes during operation. Since the PEM fuel cell produces current with an exothermic reaction, the cell temperature increases in direct proportion to the current drawn. High temperatures cause dehydration of the membrane and permanently damage the catalysts in the electrodes. Therefore, simultaneous adjustment of the cell temperature to the current drawn during operation will have a positive effect on cell performance and durability. To achieve this, first of all, it is necessary to examine the differential form of the Gibbs free energy in order to understand how the reversible voltage changes with temperature:

$$\mathrm{d}G = -S\mathrm{d}T + V\mathrm{d}p \tag{8}$$

This expression can also be written:

$$\left(\frac{\mathrm{d}G}{\mathrm{d}T}\right)_p = -S \tag{9}$$

The expression for the molar reaction amount takes the form:

$$\left[\frac{\mathrm{d}(\Delta\hat{g})}{\mathrm{d}T}\right]_p = -\Delta\hat{s} \tag{10}$$

Since the relationship of the Gibbs free energy to the reversible cell voltage is as follows [31]:

$$\Delta\hat{g} = -nFE \tag{11}$$

Combining eq. (10) and eq. (11) gives us how the reversible cell voltage changes with temperature:

$$\left(\frac{\mathrm{d}E}{\mathrm{d}T}\right)_p = \frac{\Delta\hat{s}}{nF} \tag{12}$$

If E_T is defined as the reversible cell voltage for any temperature T, it can be calculated:

$$E_T = E^0 + \frac{\Delta\hat{s}}{nF}(T - T_0) \tag{13}$$

As can be seen from eq. (13), if $\Delta\hat{s}$ is positive for a chemical reaction, E_T is directly proportional to temperature. If $\Delta\hat{s}$ is negative, the reversible fuel cell voltage decreases with increasing temperature. Take the H_2-O_2 fuel cell as an example. If H_2O is obtained as a product in the gas phase, the entropy change of the reaction $\Delta\hat{s}_{\mathrm{reaction}}$ can be calculated as

–44.34 J/molK from the thermodynamic property tables. In this case, depending on the changing temperature, the cell voltage becomes [32]:

$$E_T = E^0 + \frac{-44.34}{(2)(96,500)}(T - T_0) \tag{14}$$

As a result, it is seen that the voltage decreases by about 23 mV for every 100 degree increase in the temperature of each cell. Kinetic losses increase with decreasing temperature. Therefore, the actual fuel cell performance increases with increasing temperature, despite the decrease in the thermodynamic reversible voltage [33].

Results and discussions

An experimental and numerical investigation was performed to observe the performance differences between steady and dynamic operating conditions. In this study temperature of cell were varied among 40-80 °C and anode and cathode RH were varied among 25%, 50%, 75%, and 100%. In order to make comparisons, first of all, all experiments and analyzes were carried out at constant values. Then, in the experiment and model study, the experiments were applied again by changing the conditions between the current drawn value and the operating conditions, considering the given mathematical relations above. Table 2 shows the variables used in this model.

Table 2. Variables used for mathematical model

Variable	Description	Unit
F = 96487	Faraday's constant	[Coulombs]
T_c = 85	Temperature	[°C]
R = 8.314	Universal gas constant	[Jmol^{-1}K^{-1}]
P_{H}^2 = 2	Pressure for H_2	[atm]
P_{air} = 2	Pressure for air	[atm]
A_{cell} = 50	Cell active area	[cm^2]
N_{cells} = 1	Number of Cells	
r = 0.19	Resistance for FC components	[Ωcm^{-2}]
Alpha = 0.5	Transfer coefficient	
Alpha1 = 0.085	Amplification constant	
$i_o = 10^{-6.912}$	Exchange current density	[A cm^{-2}]
i_l = 1.4	Limiting current density	[A cm^{-2}]
Gf_{liq} = –228170	Gibbs function (for liquid form)	[Jmol^{-1}]
k = 1.1	Mass transport constant	

Effect of temperature

The operating temperature of PEMFC should be around 80 °C in theory. Deviation from the optimal range decreases the efficiency and may causes damage to the membrane. Therefore, in order to observe the effect of temperature, it was studied at constant temperature

values of 40 °C to 80 °C, both in the mathematical model and in the experimental measurements. Figure 2(a) shows the experimental results and the fig. 2(b) shows the mathematical model results. Both mathematical and experimental results indicate that the power production efficiency of the cell is increased with the increase of operational temperature. The effect of temperature on reversible cell voltage has a somewhat complex mechanism. As explained above, the reversible voltage drops with increasing temperature. However, the kinetic losses increase with decreasing temperature. The effects of the mentioned interactions on performance are seen in both experimental and mathematical model results. Cell performance increased with increasing temperature. Another point to be considered is the high current density region. Another aspect that should be carefully examined is the high current density region. Since the reaction rate is increased at values higher than 1 A/cm^2, the amount of heat produced in the cell also increases. In this case, the fuel cell will have operated above the desired temperature value. This effect is more evident especially as the number of cells in the stack increases. In both experimental, fig. 2(a), and mathematical model, fig. 2(b), cell performance was found to be somewhat lower than expected in high current density regions.

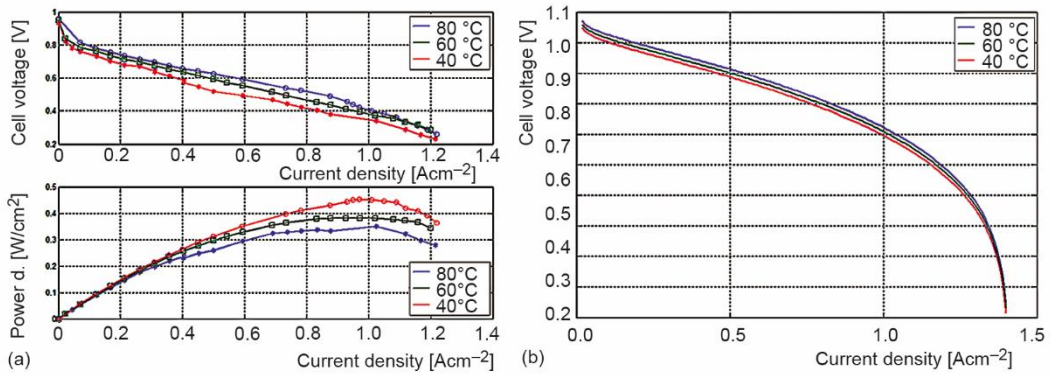

Figure 2. Experimental results for different temperatures (a), temperature values kept constant during the experiments (pressure H_2/air = 2/2 atm, RH = 100%) and effect of operating temperature on fuel cell *i-V* curve, mathematical model results (b) (*for color image see journal web site*)

In order to prevent this situation, in the experimental study, after the current drawn from the cell exceeded 0.8 A/cm^2, the cell temperature was gradually decreased by 2 °C for every 0.1 A. Experimental results are shown in fig. 3(a) and mathematical results are shown in fig. 3(b) When the figures were examined, it was seen that the performance did not decrease in the high current density regions in both mathematical and experimental results. Despite the increased heat generation with the increase in the reaction rate in the cell, adjusting the temperature depending on the current drawn value had a positive effect on the fuel cell performance outputs.

Effect of relative humidity

Effect of humidification on fuel cell outputs is observed in this section. Adequate membrane hydration was achieved by humidifying the reactants before being fed into the stack. The RH of the reactant gases was adjusted by the temperature control unit. The RH ratios were kept equal during the experiments for both of the anode and cathode gases.

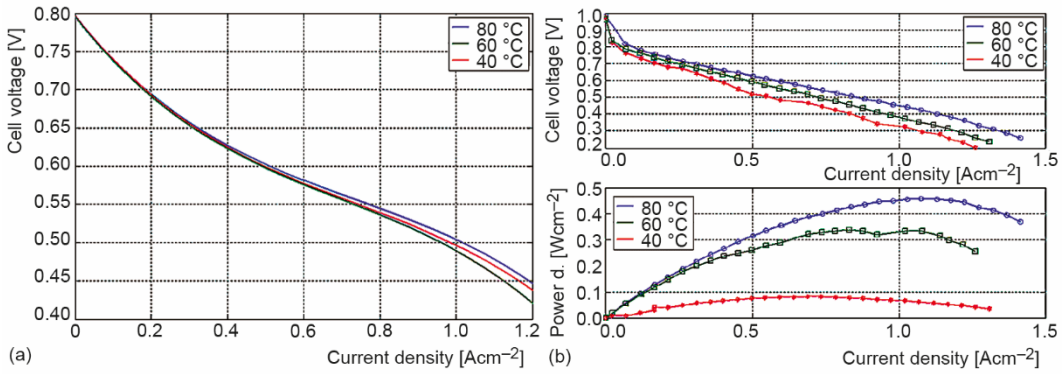

Figure 3. Mathematical model results for variable temperature values (a), constant temperatures up to 0.8 A/cm^2 were applied; after this value, the temperature was reduced by 2 °C in the MATLAB code for every 0.1 A value increased and (b) experimental results for variable temperature values, constant temperatures up to 0.8 A/cm^2 were applied; after this value, the temperature was reduced by 2 °C with the temperature control unit for every 0.1 A value increased (pressure H_2/air = 2/2 atm, RH = 80%) (*for color image see journal web site*)

The ohmic resistance area is reached as the current density rises. For a well-built PEM fuel cell stack, the ionic transfer resistance makes up the majority of the fuel cell's overall ohmic resistance in this region. While examining the effect of RH, the cell temperature is kept constant. In this regime, the amount of water in the membrane mostly determines its ionic conductivity. So, by examining the changing ohmic resistance, it is possible to determine the history of membrane hydration and, consequently, the water content of the membrane. In the high current density region, the decrease in cell voltage is called the concentration loss region. In addition, the voltage drop in this region also depends on the cell's water remove capability. With optimum humidification, the voltage drop in this region can be kept to a minimum. Figure 4(a) and fig. 4(b) show the effect of the cell constant relative humidity values on the performance for both mathematical model and experimental study, respectively.

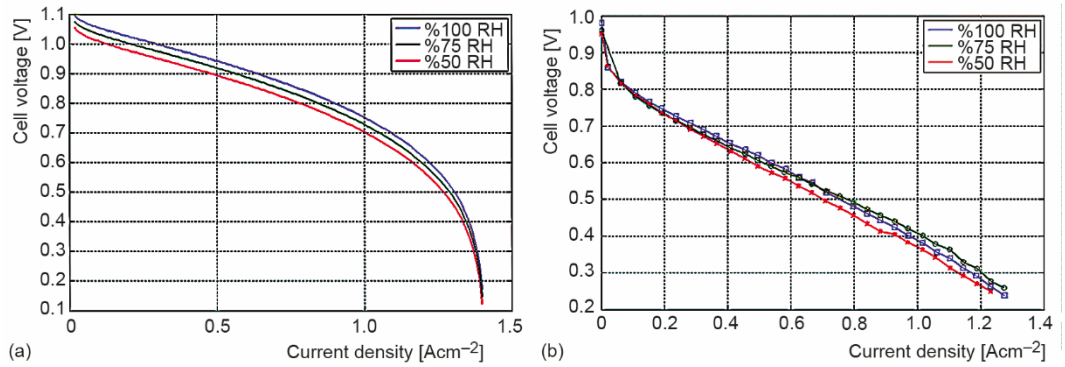

Figure 4. Numerical simulation results for three different RH ratios (a) and experimental measurement results for three different RH ratios (b) (*for color image see journal web site*)

When fig. 4 is examined, it is observed that the increase in RH value has a positive effect on fuel cell performance. However, when the behavior of the cell is examined carefully,

it is seen that the RH value causes different behavior at current density values higher than 0.6 A/cm^2. With the increase of current density, a decrease in cell voltage is observed for 100% RH value. Likewise, it can be seen that the experimental result fig. 4(b) with 75% RH gives better results in high current density phases. The reason for this is that the increase in the current value produced by the fuel cell means that the reaction rate increases. Considering that the cell operates at 60 °C, the amount of liquid water produced also increases. Although water is indispensable for the ion transmission mechanism inside the cell, excess water negatively affects cell performance. The excess water that cannot be discharged causes flooding, which results in the catalyst particles in the electrode layers being surrounded by water. As a result, as the reactants cannot come into contact with the catalysts, the amount of reaction decreases and as seen in the experimental results, the cell performance is adversely affected at high current density. It is clearly seen that 100% RH value is more ideal for low current density values and 75% RH value is more ideal for medium and high current density values. It is understood that the RH value, which will be suitable for the entire current density value range in which the fuel cell will operate, should not be a fixed value, but values that vary according to the current. Therefore, the experiments were performed again by adjusting the RH value according to the current drawn from the fuel cell.

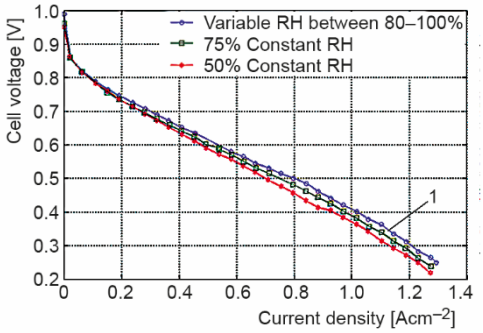

Figure 5. Experimental results for variable and constant RH values, constant RH up to 0.6 A/cm^2 were applied; after this value, the RH was reduced by 2,5% with the humidity and temperature control unit for every 0.1 A value increased (pressure H_2/air = 2/2 atm, cell temperature = 60 °C)
(*for color image see journal web site*)

In fig. 5, RH ratios of 50% and 75% were kept constant. however, in the other measurement (blue line – 1), the RH value was gradually reduced from 100% to 80%. The value of 0.6 A/cm^2 was chosen as the beginning of the reduction of the RH value. The reason for this is seen in the test with 100% RH. Since the amount of liquid water produced in the fuel cell depends on the increasing current value, a decrease was observed in the constant RH experiment after this value. To prevent this decrease, the RH value was decreased by 2.5% for every 0.1 A/cm^2 value that increased after 0.6 A/cm^2. This reduction was continued until the RH value was 80% when 1.4 A/cm^2 current was drawn from the cell. As a result, it has been observed that decreasing the RH value depending on the increasing current density has a positive effect on the fuel cell performance. When the *i*-*V* curves in fig. 4 and fig. 5 are compared, it is clear that the decrease in the ohmic and concentration losses region is not experienced in the variable RH approach. The reason for this performance improvement in the fuel cell is that the amount of reactant consumed increases with the increasing current demand. As a result, liquid water, which is one of the products of the H_2 reaction, is produced more in high current density regions. The produced liquid water cannot be discharged and covers the catalyst particles on the electrodes. The reactants that cannot reach the catalyst particles cannot enter the reaction at the desired level and a decrease in the *i*-*V* curve is experienced. The RH

value, which was gradually reduced against the increasing current density, eliminated this negative effect and prevented the decrease in fuel cell performance.

Conclusions

In this study, cell temperature and RH, which are the most important operating conditions affecting the PEMFC performance, were investigated. The experiments were conducted in a cell with a 50 cm^2 active area with serpentine flow channel. In the MATLAB program, a mathematical model was used to validate the experimental results. In all experimental measurement and mathematical models, the aforementioned operating conditions were kept constant and changed at the values given in the table below according to the current drawn from the cell.

The PEMFC, which should theoretically operate at around 80 °C, exceeds this temperature by generating more heat when high current is drawn. Increased temperature is not desirable for membranes and catalysts. In the experimental results, it was observed that the performance of the cell operating at 80 °C decreased somewhat in high current density regions. Therefore, in response to the increased current value, the gradual reduction of the cell temperature by means of the temperature control unit has improved the result.

Similarly, decreasing the RH ratio due to the increasing amount of current had a positive effect on the cell performance, especially in the high current density region. High moisture content increases the ion conduction capability of the membrane and reduces ohmic losses. However, 100% RH rate causes flooding in case of high current draw from the cell and adversely affects the cell outputs. This negative effect was also eliminated by adjusting the RH ratio according to the values given in tab. 3 according to the increasing current value.

Table 3. Variable operating condition values according to current density

Operating condition	Value								
Current density [Acm^{-2}]	0.6	0.7	0.8	0.9	1.0	1.1	1.2	1.3	1.4
Cell Temperature [°C]	80	80	80	78	76	74	72	70	68
RH ratio [%]	100	97.5	95	92.5	90	87.5	85	82.5	80

All adjustments (cell temperature and RH) made in this study were changed manually in the experimental study. Setting these values electronically in a software management is seen as a good working suggestion.

Nomenclature

c_p – heat capacity of mixture, [$Jkg^{-1}K^{-1}$]
D_λ – water diffusivity in ionomer, [$m^2\ s^{-1}$]
E_T – reversible cell voltage, [V]
F – Faraday constant, [$Cmol^{-1}$]
G – Gibbs free energy, [Joule]
k – thermal conductivity, [$Wm^{-1}K^{-1}$]
M_m – molar mass, [$kgmol^{-1}$]
n – electrons transferred
p – fluid pressure, [Pa]
$\hat{s}$ – entropy, [$Jmol^{-1}K^{-1}$]
S_e – energy source
S_m – momentum source
$S_{s,i}$ – species sources
T – temperature, [K]
v – velocity, [ms^{-1}]

Greek symbols

μ – viscosity, [$kgm^{-1}s^{-1}$]
ρ – density, [kgm^{-3}]
ε – porosity
λ – membrane water content

References

[1] Kahraman, H,. Orhan, M. F., Flow Field Bipolar Plates in a Proton Exchange Membrane Fuel Cell: Analysis & modeling, *Energy Convers. Manag., 133* (2017), Feb., pp. 363-834
[2] Ozer, S., Effects of Alternative Fuel Use in a Vehicle with TSI (Turbocharged Direct-Injection Spark-Ignition) Engine Technology, *Int. J. Green Energy, 18* (2021), 12, pp. 1309-1319
[3] Kahraman, H., *et al.*, The Corrosion Resistance Behaviors of Metallic Bipolar Plates for PEMFC Coated with Physical Vapor Deposition (PVD): An Experimental Study, *Arab J. Sci. Eng., 41* (2016), Feb., pp. 1961-1968
[4] Ozer, S., Doğan, B., Thermodynamic Analyzes in a Compression Ignition Engine Using Fuel Oil Diesel Fuel Blends, *Thermal Science, 26* (2022), 4, pp. 3079-3088
[5] Chen, M., *et al.*, Research Progress of Catalyst Layer and Interlayer Interface Structures in Membrane Electrode Assembly (MEA) for Proton Exchange Membrane Fuel Cell (PEMFC) System, *ETransportation, 5* (2020), Aug., 100075
[6] Liu, J., *et al.*, Chemical LOOPING INDUCED CH_3OH-H_2-PEMFC Scheme for Fuel Cell Vehicle: Parameter Optimization and Feasibility Analysis, *J. Power Sources, 479* (2020), Dec., 228790
[7] Liu, S., *et al.*, Study on the Performance of Proton Exchange Membrane Fuel Cell (PEMFC) with Dead-Ended Anode in Gravity Environment, *Appl. Energy, 261* (2020), Mar., 114454
[8] Azarafza, A., *et al.*, Comparative Study of Conventional and Unconventional Designs of Cathode Flow Fields in PEM Fuel Cell, *Renew. Sustain. Energy Rev., 116* (2019), Dec., 109420
[9] Kahraman, H., Coban, A., Performance Improvement of a Single Pem Fuel Cell Using an Innovative Flow Field Design Methodology, *Arab. J. Sci. Eng., 45* (2020), Jan., pp. 5143-5152
[10] Anyanwu, I. S., *et al.*, Comparative Analysis of Two-Phase Flow in Sinusoidal Channel of Different Geometric Configurations with Application to PEMFC, *Int. J. Hydrog. Energy, 44* (2019), 26, pp. 13807-13819
[11] Zheng, Z., *et al.*, Design of Gradient Cathode Catalyst Layer (CCL) Structure for Mitigating Pt Degradation in Proton Exchange Membrane Fuel Cells (PEMFC) Using Mathematical Method, *J. Power Sources, 451* (2020), Mar., 227729
[12] Lee, D., Bae, J., Visualization of Flooding in a Single Cell and Stacks by Using a Newly-Designed Transparent PEMFC, *Int. J. Hydrog. Energy, 37* (2012), 1, pp. 422-435
[13] Isanaka, S. P., *et al.*, Design Strategy for Reducing Manufacturing and Assembly Complexity of Air-Breathing Proton Exchange Membrane Fuel Cells (PEMFC), *J. Manuf. Syst., 38* (2016), Jan., pp. 165-171
[14] Min, X., *et al.*, Preliminary Experimental Study of the Performances for a Print Circuit Board Based Planar PEMFC Stack, *Int. J. Hydrog. Energy, 47* (2022), 8, pp. 5599-5608
[15] Yu, Y., *et al.*, Thermal Management System for Liquid-Cooling PEMFC Stack: From Primary Configuration to System Control Strategy, *ETransportation, 12* (2022), May, 100165
[16] Niu, H., *et al.*,. Quantitative Analysis on Cold Start Process of a PEMFC Stack with Intake Manifold, *Int. J. Hydrog. Energy, 47* (2022), 4, pp. 2647-2661
[17] Wu, S.-J., *et al.*, Parametric Analysis of Proton Exchange Membrane Fuel Cell Performance by Using the Taguchi Method and a Neural Network, *Renew. Energy, 34* (2009), 1, pp. 135-144
[18] Solehati, N., *et al.*, Optimization of Operating Parameters for Liquid-Cooled PEM Fuel Cell Stacks Using Taguchi Method, *J. Ind. Eng. Chem., 18* (2012), 3, pp. 1039-1050
[19] Jia, Y., *et al.*, A Parametric Comparison of Temperature Uniformity and Energy Performance of a PEMFC Having Serpentine Wavy Channels, *Int. J. Energy Res., 43* (2019), 7, pp. 2722-2236
[20] Salva, J. A., *et al.*, Experimental Validation of the Polarization Curve and the Temperature Distribution in a PEMFC Stack Using a one Dimensional Analytical Model, *Int. J. Hydrog. Energy, 41* (2016), 45, pp. 20615-20632
[21] Kim, B., *et al.*, Effects of Cathode Channel Size and Operating Conditions on the Performance of Air-Blowing PEMFCs, *Appl. Energy, 111* (2013), Nov., pp. 441-448
[22] Chen, X., *et al.*, Active Disturbance Rejection Control Strategy Applied to Cathode Humidity Control in PEMFC System, *Energy Convers. Manag., 224* (2020), Nov., 113389
[23] Santarell, M. G., Torchio, M. F., Experimental Analysis of the Effects of the Operating Variables on the Performance of a Single PEMFC, *Energy Convers. Manag., 48* (2007), 1, pp. 40-51
[24] Hu, G., *et al.*, Optimization and Parametric Analysis of PEMFC Based on an Agglomerate Model for Catalyst Layer, *J. Energy Inst., 87* (2014), 2, pp. 163-174

[25] Wang, Y., *et al.*, Optimization of Reactants Relative Humidity for High Performance of Polymer Electrolyte Membrane Fuel Cells with Co-Flow and Counter-Flow Configurations, *Energy Convers. Manag., 205* (2020), 112369
[26] Bilgili, M., Sivrioglu, M., 3D Numerical AnalySIS of Pem Fuel Cell at Different Mea Thicknesses and Operating Pressure Conditions, *J. Fac. Eng. Archit. GAZI Univ., 31* (2016), 1, pp. 51-63
[27] Gunduz, T., Demircan, T., Numerical Analysis of the Effects of Current Collector Plate Geometry on Performance in a Cylindrical PEM Fuel Cell, *Int. J. Hydrog. Energy, 47* (2022), 39, pp. 17393-17406
[28] Solati, A., *et al.*, Numerical Investigation of the Effect of Different Layers Configurations on the Performance of Radial PEM Fuel Cells, *Renew. Energy, 143* (2019), Dec., pp. 1877-1889
[29] Xie, B., *et al.*, Three-Dimensional Multi-Phase Model of PEM Fuel Cell Coupled with Improved Agglomerate Sub-Model of Catalyst Layer, *Energy Convers. Manag., 199* (2019), Nov., 112051
[30] Kanchan, B. K., *et al.*, Numerical Investigation of Multi-Layered Porosity in the Gas Diffusion Layer on the Performance of a PEM Fuel Cell, *Int. J. Hydrog. Energy, 45* (2020), 41, pp. 21836-21847
[31] Vasilyev, A., *et al.*, Component-Based Modelling of PEM Fuel Cells with Bond Graphs, *Int. J. Hydrog. Energy, 42* (2017), 49, pp. 29406-29421
[32] Pukrushpan, J. T., *et al., Control of Fuel Cell Power Systems: Principles, Modeling, Analysis and Feedback Design*, Springer Science & Business Media, New York, USA, 2004
[33] O'Hayre, R., *et al., Fuel Cell Fundamentals*, John Wiley & Sons, New York, USA, 2016

Paper submitted: March 21, 2023
Paper revised: April 11 2023
Paper accepted: May 4, 2023